iScience

Article

Microglia and its P2RY12 receptors regulate seizure severity

Graphical abstract

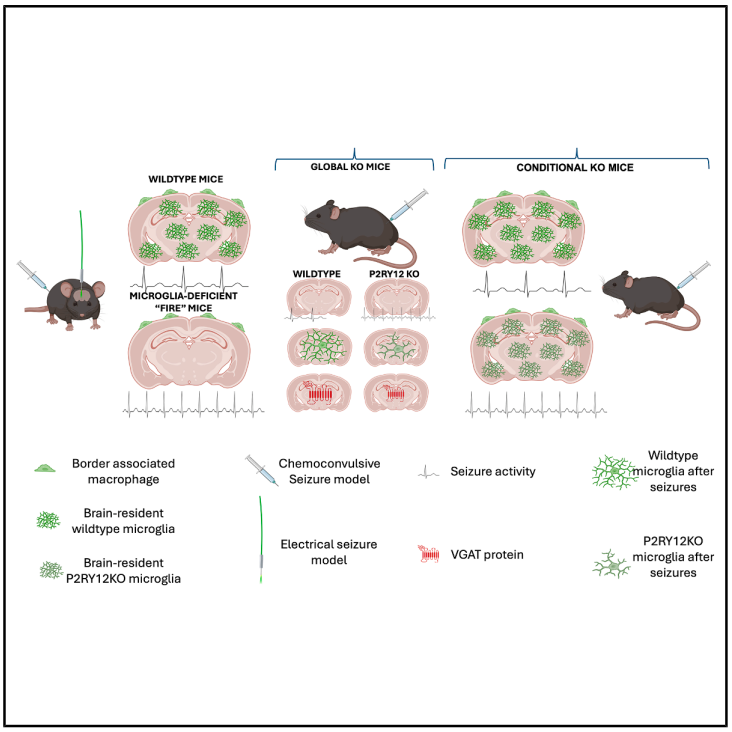

Highlights

- Microglia-selective depletion in FIRE KO mice show exacerbated seizures
- Microglial P2RY12 deletion leads to exacerbated chemoconvulsive seizures
- A genetic P2RY12 deficiency alters microglial morphologies in seizures
- A genetic P2RY12 deficiency impairs neuronal inhibitory tone in seizures

Authors

Leigh Ellen Fremuth, Synphane Gibbs-Shelton, Madison Doceti, ..., Sophia Cheng, Edward Perez-Reyes, Ukpong B. Eyo

Correspondence

qgc6xt@virginia.edu (L.E.F.), ube9q@virginia.edu (U.B.E.)

In brief

neurology; neuroscience; cell biology

Fremuth et al., 2026, iScience *29*, 116563
July 17, 2026
https://doi.org/10.1016/j.isci.2026.116563

CellPress

iScience

CellPress
OPEN ACCESS

Article

Microglia and its P2RY12 receptors regulate seizure severity

Leigh Ellen Fremuth,[1,2,4,7,*] Synphane Gibbs-Shelton,[1,3,7] Madison Doceti,[5] Aida Oryza Lopez-Ortiz,[1,2,5,6] Abigayle Duffy,[1,2,4,5,6] William A. Mills III,[1,2,4] Ronald P. Gaykema,[3] Kiran Singh,[3] Audrey Nguyen,[2] Sophia Cheng,[2] Edward Perez-Reyes,[3] and Ukpong B. Eyo[1,2,4,5,6,8,*]

[1]Brain Immunology and Glia Center, University of Virginia, Charlottesville, VA, USA
[2]Department of Neuroscience, University of Virginia, Charlottesville, VA, USA
[3]Department of Pharmacology, University of Virginia, Charlottesville, VA, USA
[4]Cardiovascular Research Center, University of Virginia, Charlottesville, VA, USA
[5]Department of Microbiology, Immunology and Cancer, University of Virginia, Charlottesville, VA, USA
[6]Neuroscience Graduate Program, University of Virginia, Charlottesville, VA, USA
[7]These authors contributed equally
[8]Lead contact
*Correspondence: qgc6xt@virginia.edu (L.E.F.), ube9q@virginia.edu (U.B.E.)
https://doi.org/10.1016/j.isci.2026.116563

SUMMARY

Microglia are possible regulators of seizures but previous employed approaches are insufficiently selective of microglial-specific manipulations. To more definitely determine microglial roles in seizure severity, we used the microglial-deficient *Csf1r*$^{\Delta FIRE/\Delta FIRE}$ mouse model where mice lack microglia but retain brain border-associated macrophages. Using two experimental paradigms, we confirm that a microglial deficiency exacerbates seizures and facilitates the likelihood of developing spontaneous recurrent seizures, indicating that microglia constrain seizure activity. To gain insights into microglial molecular regulators of seizure severity, we examined P2RY12 contributions and demonstrate that a loss of P2RY12 increased seizure severity in both global and microglial-specific knockout mice indicating that microglia suppress seizure severity. During seizures, P2RY12-deficient microglia displayed altered process complexity, accompanied by increased neuronal activation and reduced inhibitory tone. These results link impaired microglial responses to heightened seizure susceptibility and network excitability. Together, we establish microglia and P2RY12 signaling as protective regulators of seizure activity.

INTRODUCTION

Statistics indicate that about 1 in 26 people will develop epilepsy in their lifetime[1–3] making it a common disorder. Epilepsy is characterized by the occurrence of seizures as its most obvious manifestation. While seizures are known to result from an imbalance in neuronal excitation and inhibition, treatment approaches that target neuron-autonomous mechanisms have remained insufficient in treating seizure disorders in many patients[4–6] raising the need for identifying alternative treatment approaches/targets that are relevant for seizure induction, maintenance, and/or termination. Of particular interest, glial cells that modulate neuronal activity are receiving increasing attention as important contributors to seizures and epilepsy.[7–9]

Emerging findings indicate that inflammatory processes contribute to seizures.[10–12] However, cell-specific assessments of neuroinflammatory contributions to seizures require further research. Among brain cells, microglia are uniquely positioned at the interface of the nervous and immune systems being the primary immunocompetent cells of the brain. Our understanding of microglial roles in seizures and epilepsy development is still at its infancy. Results indicate complex roles for microglia with some studies suggesting seizure-limiting[13–17] and others suggesting seizure-promoting roles.[18–24] However, appropriate tools are required for precise investigation and the elucidation of relevant, targetable mechanisms.

Recently, a powerful tool for microglial studies was developed in the form of the generation of Csf1r$^{\Delta FIRE/\Delta FIRE}$ (FIRE knockout or KO) mouse, where deletion of the fms-intronic regulatory element (FIRE) at the *Csf1r* locus results in the prevention of microglial development without affecting other brain macrophage populations.[25] This mouse model, therefore, provides a powerful microglial-selective model to assess microglial roles in experimental seizure contexts. Interestingly, a recent study suggested that synaptic maturation and seizure susceptibility were unaltered in FIRE KO mice during development.[26] This finding is not congruent with previous literature that suggested microglia play active and protective roles during status epilepticus and during the chronic phase of spontaneous recurring seizures in mice[15] and a zebrafish developmental Dravet syndrome model of genetic seizures.[17] Moreover, the FIRE KO mice have not

been used to interrogate microglial contribution to experimental seizures in adulthood.

Furthermore, whereas some studies define a protective role of the microglia in restricting the severity of seizures through various seizure models, identifying molecular mediators controlling microglial seizure-regulating activities is important for developing therapeutic interventions. Among candidates, the P2RY12 receptor is a microglial signature gene[27] and regulates microglial-neuronal communication through sensing extracellular ADP during neuronal activity from hyperactive neurons to facilitate restoration to homeostatic states.[28–33] Lack of P2RY12 has been implicated in defective microglial chemotaxis,[34] a defective synaptic management,[35,36] and increased network excitability,[37,38] implying that the P2RY12 may provide a link of mechanisms between microglial surveillance, microglial-neuronal interactions, and seizure inhibition.

In this study, we interrogate microglial and P2RY12-specific roles in experimental seizures. First, with FIRE KO mice, we establish a neuroprotective role for microglia in modulating seizure severity in both chemoconvulsive (kainic acid [KA] induced) seizures and electrical kindling seizure paradigms. Second, using P2RY12 global and constitutive microglial knockout lines, we identify a role for microglial P2RY12 in the seizure-related suppression attributed to microglia. Finally, we correlate this role with alterations in microglia process complexity, neuronal cFos activity, and inhibitory vesicular GABA transporter (VGAT) synaptic expression. Thus, we highlight alterations by which microglial P2RY12 preserve network integrity with seizures.

RESULTS

"FIRE" KO mice show exacerbated chemoconvulsant seizures

In previous work, we used a pharmacological microglial depletion model to assess microglial contributions to seizures in three seizure paradigms, including chemoconvulsive, electrical, and temperature-induced febrile seizure models. In those paradigms, we reported exacerbated seizures in mice with pharmacological microglial elimination.[15] However, pharmacological inhibition of CSF1R using PLX3397, while efficiently eliminating microglia, also targets brain border-associated macrophages (BAMs) leaving the possibility that effects seen with that pharmacological approach may be a result of these BAMs. More selective approaches are therefore needed to ascertain microglial roles in experimental seizure paradigms.

To investigate the specific role of microglia in seizure regulation, we utilized Csf1r$^{\Delta FIRE/\Delta FIRE}$ (hereafter referred to as "FIRE KO") mice, a genetically engineered model that lacks brain microglia due to deletion of the FIRE within the *Csf1r* gene.[25] Unlike pharmacological depletion approaches[39] which affect BAM populations,[39,40] the FIRE KO model provides a selective and permanent loss of microglia while preserving brain BAMs densities.[25] Given that FIRE KO mice lack microglia but retain other brain macrophage populations, this model allows us to isolate the role of microglia specifically, independent of brain BAMs, in modulating seizure severity. Using this approach, we examined seizure susceptibility across two seizure paradigms in adult mice.

We crossed FIRE KO mice with CX3CR1-GFP mice to generate CX3CR1$^{GFP/+}$ littermates that would allow for the visualization of myeloid cells by GFP. We confirmed the absence of microglia in the brains of FIRE KO mice compared to wild type (FIRE WT) and FIRE heterozygous (FIRE HET) littermate mice (Figures 1A–1C). The quantification of GFP$^+$ microglia between FIRE WT and FIRE HET was indistinguishable, while FIRE KO had no microglia (Figure 1D), consistent with previous reports.[25] The only GFP$^+$ cell detected in FIRE KO mice were BAMs. These CD206$^+$ BAMs were present in similar numbers in the three genotypes (Figures S1A and S1B), also consistent with previous reports.[25] Interestingly, microglia in FIRE WT and FIRE HET mice showed indistinguishable morphologies when assessed by a Scholl analysis (Figures 1E and 1F). The selective microglia deficiency in FIRE KO mice allowed us to investigate the impact of microglial absence on chemoconvulsive seizure severity.

Chemoconvulsive seizures were induced by KA treatment (IP, 24 mg/kg), and seizure severity was quantified using a modified Racine seizure scoring[22] scheme over time. FIRE KO mice exhibited persistently high seizure scores during the 3 h monitoring period and significantly increased peak seizure scores when compared to WT and HET controls (Figures 1G and 1H). This suggests a heightened susceptibility to chemoconvulsive seizures in the absence of microglia. Moreover, animal survival analysis revealed a reduced probability of survival in FIRE KO mice following seizure induction when compared to HET littermates (Figure 1I), highlighting a critical role for microglia in mitigating seizure-induced mortality. These findings support the hypothesis that microglia play an essential neuroprotective role during seizures by maintaining neural homeostasis, as we and others have previously suggested.[14,15,17,32,41]

Because previous studies[15] showed similar results using a pharmacological approach to eliminate microglia with PLX3397[42] that targets both microglia and brain BAMs,[43] it is possible that these macrophages that persist in FIRE KO mice also contribute to seizure susceptibility to KA. To evaluate whether these macrophage populations contribute to the increased seizure severity observed in FIRE KO mice, we treated FIRE KO mice with PLX3397 (or control) for 7 days to further deplete macrophages and confirmed that this procedure eliminated CD206$^+$ BAMs in "FIRE+PLX" mice (Figures S1A and S1B). Seizure severity scores were compared between FIRE KO mice "FIRE+PLX" mice. Notably, "FIRE+PLX" mice exhibited seizure severity scores like FIRE KO mice, indicating that additional macrophage populations beyond microglia do not contribute significantly to seizure severity in this KA model (Figures S1C–S1E). Therefore, consistent with the conclusion from our prior findings,[14] studies in FIRE KO mice reveal that microglia regulate seizure susceptibility in a neuroprotective manner.

"FIRE" KO mice show exacerbated electrical seizures

Our findings contrast with a recent study that examined seizure susceptibility in a PTZ model using FIRE mice and reported no significant roles for microglia in that context during development.[26] Therefore, to determine whether microglial contributions to seizure susceptibility are limited to chemoconvulsive seizure models, we expanded our studies to an electrical kindling model.

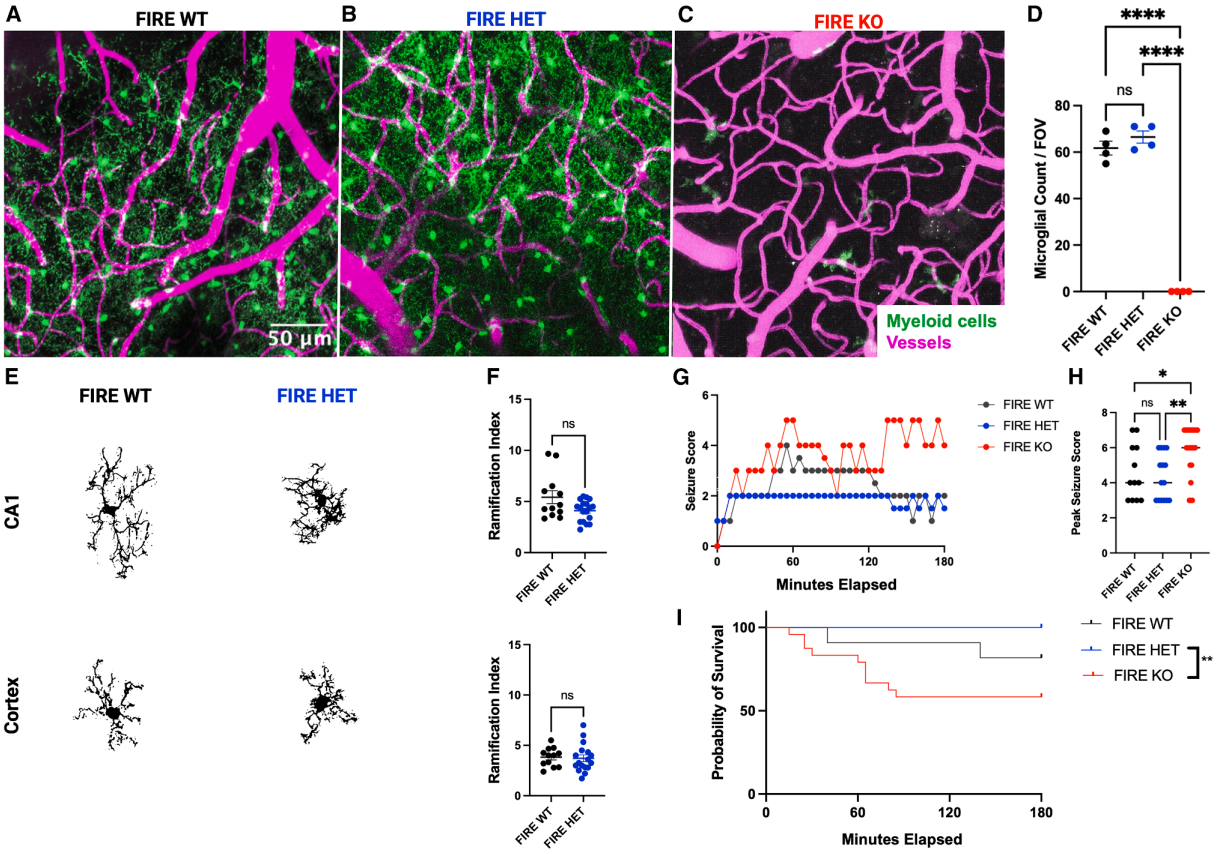

Figure 1. FIRE knockout mice are more susceptible to kainic acid-induced seizures

(A–C) Representative *in vivo* two photon images showing microglial depletion in Csf1r$^{\Delta FIRE/\Delta FIRE}$ (FIRE KO) mice compared to wild-type (FIRE WT) and Csf1r$^{\Delta FIRE/+}$ (FIRE HET) mice. CX3CR1$^{GFP/+}$ (green) marks microglia, while rhodamine B (magenta, 50–100 µL at 1 mg/ml IP) highlights the vasculature.

(D) Quantification of microglial numbers in littermate Csf1r$^{+/+}$ (FIRE WT), Csf1r$^{\Delta FIRE/+}$ (FIRE HET), and Csf1r$^{\Delta FIRE/\Delta FIRE}$ (FIRE KO) mice.

(E and F) Representative microglial images (E) and morphological quantification (F) of microglia from FIRE WT and FIRE HET mice.

(G and H) Seizure severity scores along a modified Racine scale over time (G) and peak seizure scores (H) In FIRE WT, FIRE HET, and FIRE KO littermate mice following KA-induced seizures.

(I) Kaplan-Meier survival curves of FIRE WT, FIRE HET, and FIRE KO littermates that underwent KA-induced seizures. n = 12–16 microglia from 2 to 3 mice each for (E) and (F). N = 12–23 per group for (G–I). Scale bars in (A) are 50 µm. Error bars represent SEM in (D) and (F). Statistical significance was determined using one-way ANOVA (D and H), and one-way ANOVA (I). *p < 0.05; **p < 0.01; ****p < 0.0001.

Specifically, kindling induces gradual neuronal hyperexcitability through repeated electrical stimulation.[44] If microglia are truly dispensable in seizure regulation, as previously suggested by the recent study,[26] we would expect no differences in kindling progression between FIRE KO and FIRE HET mice. However, when FIRE KO mice were kindled, they required fewer stimulations to get to stage 5 seizures (bilateral clonus with loss of balance) compared to FIRE HET littermate mice (Figures 2A and 2B). Kindling of FIRE knockout mice also increased the fraction of mice that developed spontaneous recurrent seizures (SRSs), leading to more frequent and severe seizures per mouse compared to the FIRE HET mice (Figures 2C and 2D). Furthermore, while ~30% (2 of 7) of HET mice showed SRSs after kindling, 100% (4 of 4) of KO mice showed SRSs. Since most strains of mice do not develop SRSs after kindling,[44] this highlights an important role for endogenous microglia in limiting spontaneous seizure generation. Therefore, our studies demonstrate that FIRE KO mice have exacerbated seizures during both chemoconvulsive and electrical kindling.

A global or microglial-specific P2RY12 deficiency exacerbates chemoconvulsive KA-induced seizures

Having established that microglia are required for limiting seizure severity in a chemoconvulsive (Figure 1) and an electrical (Figure 2) seizure model using FIRE mice, we next sought to investigate possible mechanisms involved in microglial protection against seizure severity. The purinergic receptor P2RY12 is a microglial-enriched molecule involved in microglial process extensions toward areas of hyperexcitability and can be considered to play an important role in microglial control of seizure

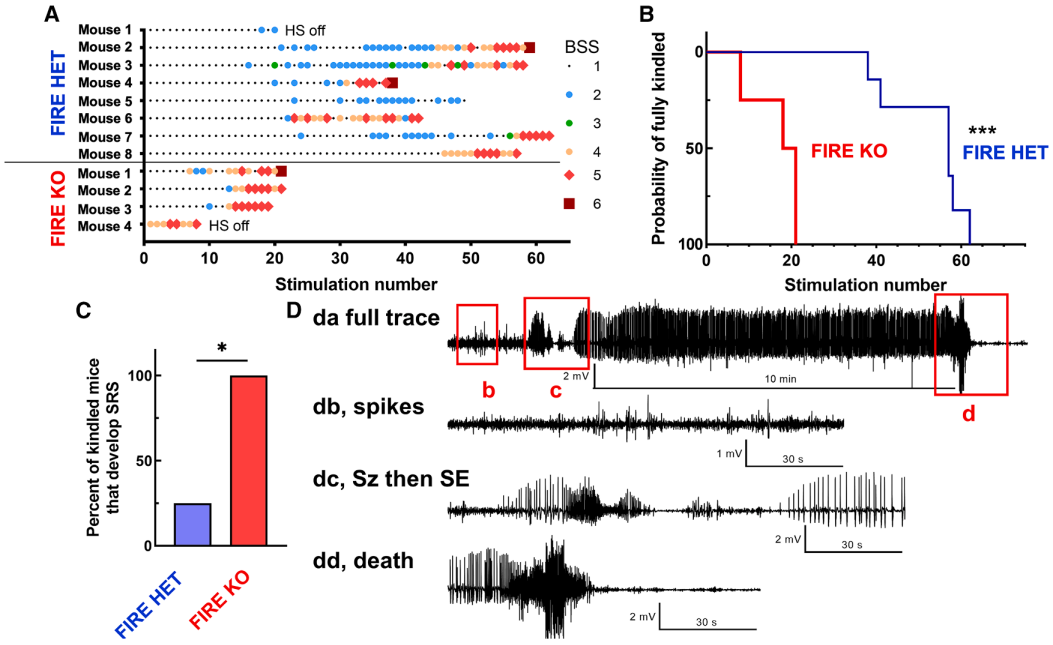

Figure 2. FIRE KO mice are more susceptible to seizures induced by electrical kindling

(A) Raster plots showing the evolution of the behavior evoked by electrical stimulation of the hippocampus in FIRE HET and FIRE KO littermates. Behavioral seizure score (BSS) key is shown on the right of (A). "HS off" denotes when the EEG recording headset fell off. Mice are considered fully kindled after electrical stimulation elicits five motor seizures with a BSS score of 5.

(B) Kaplan-Meier plot of the number of electrical stimulations required to reach the fully kindled state in FIRE HET and FIRE KO littermates.

(C) The number of mice that developed spontaneous recurrent seizures after kindling.

(D) Representative EEG traces from a FIRE KO mouse. da shows the final 960 s of EEG from mouse RF974. Red boxes show the regions expanded in db-dd. db shows high amplitude spikes in the EEG riding a baseline of high frequency/low amplitude spikes. dc shows an example of the EEG transitioning into a high frequency/high amplitude seizure, followed by a short post-ictal depression. This transitions into a 10-minute-long seizure, which fulfills the definition of status epilepticus (SE). dd, SE ends with a discrete seizure and death. $N = 4$ Hets and 7 KO littermates. Statistical analysis in (B) by Mantel-Cox indicates $p = 0.0005$, and (C) by Chi-square, $p = 0.0143$. $^{*}p < 0.05$; $^{***}p < 0.001$.

intensity.[32,41] In previous work, we had tested the role for P2RY12 in chemoconvulsive seizures using global KO mice.[32] However, in that study, littermates were not used raising possibilities of differences that may result from genetic strains. To overcome this and more conclusively test for a role for P2RY12, we assessed the seizure susceptibility in global P2RY12 knockout (gKO) and WT littermates after KA treatment. Seizures persisted in gKO mice compared to their WT littermates over 3 h and there was a significantly higher peak seizure score in P2RY12 KO mice compared to WT littermates (Figures 3A and 3B). Furthermore, the survival curves also showed that there was reduced mortality in gKO mice compared to WT littermates with KA treatment (Figure 3C). These results are consistent with our previous work suggesting roles for P2RY12 in seizure susceptibility.[32]

Nevertheless, because P2RY12 is also expressed in circulating blood platelets, where it regulates ADP-dependent aggregation and thrombosis,[45] it remained unclear whether the heightened seizure severity observed in global knockout mice resulted from the loss of microglial P2RY12 specifically or from broader systemic effects including for example platelet dysfunction. To resolve this ambiguity, we next utilized a microglia-specific constitutive P2RY12 KO model to determine whether loss of P2RY12 within microglia alone is sufficient to exacerbate seizure outcomes using a microglia-specific conditional knockout mouse model (P2RY12 $^{fl/fl}$;Cx3cr1$^{Cre/+}$), hereafter referred to as P2RY12 cKO mice and littermate P2RY12^{flf+};Cx3cr1$^{Cre/+}$ mice, hereafter referred to as P2RY12 cWT mice. In the cKO mice, P2RY12 expression was reduced in microglia (Figures 3D and 3E). Consistent with a selective loss of P2RY12 loss in microglia without effect on platelets, a bleeding assay on cWT, cKO, and gKO mice revealed significantly increased bleeding times only in the gKOs (Figure 3F) indicating preserved platelet P2RY12 function in cKO mice.

Turning to KA-induced seizures, we again report a significantly increased peak seizure scores in P2RY12 cKO mice compared to littermate cWT mice (Figures 3G and 3H). However, while the seizure severity phenotype for cKOs was consistent with that seen in gKOs, the cKOs did not show significantly different mortality rates compared to their cWT controls (Figure 3I). These data collectively validate the essential role of microglial P2RY12 signaling in regulating neuronal hyperexcitability in response to KA-induced seizures.

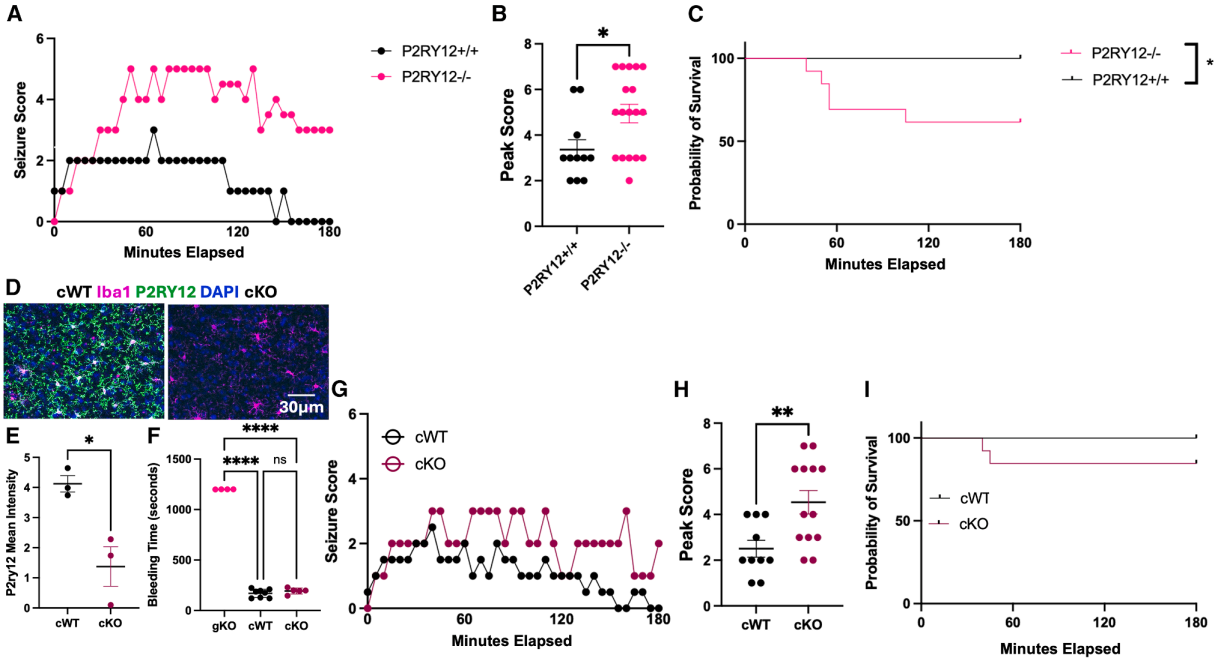

Figure 3. P2RY12 signaling in microglia is required for seizure suppression

(A) Time course of modified Racine seizure scores in P2RY12-deficient mice.

(B) Quantification of peak seizure score in P2RY12$^{-/-}$ mice ($p < 0.05$, unpaired t test).

(C) Kaplan-Meier survival analysis of survival probability in P2RY12$^{-/-}$ mice ($p < 0.05$, log rank test). $N = 11–18$ mice each.

(D) Representative confocal images of IBA1 (green) and P2RY12 (magenta) immunostaining in cWT(P2RY12 $^{fl/fl}$:CX3CR1$^{Cre/+}$) and conditional knockout cKO (P2RY12 $^{fl/fl}$:CX3CR1$^{Cre/+}$) mice confirm selective microglial deletion of P2RY12.

(E) Quantification of P2RY12 mean fluorescence intensity in cWT and cKO mice (unpaired t test). $N = 3$ mice each.

(F) Tail bleeding assay comparing platelet function across genotypes confirming microglia-specific targeting ($p < 0.0001$, one-way ANOVA with Tukey's post hoc test). $N = 4–8$ mice each.

(G–I) Modified Racine seizure scores overtime of cWT and cKO (G), peak seizure score (H, $p < 0.01$), and Kaplan-Meier survival analysis (I). $N = 10–13$ mice each. Scale bars in (D) are 30 μm. Error bars represent SEM in (B) and (H). Statistical significance was determined using Student's t test (B, E, and H), one-way ANOVA (F), and two-way ANOVA (I). *$p < 0.05$; **$p < 0.01$; ****$p < 0.0001$.

P2RY12 signaling maintains microglial ramification in response to KA

Microglial ramification, the degree of process branching and arborization, is considered a major marker of microglial homeostasis and responsiveness to changes in the surrounding tissue. Ramified microglia are constantly surveying the brain parenchyma by extending and retracting their processes to maintain balance.[46,47] We first conducted microglial tissue surveillance measurements and confirmed that global P2RY12 WT, HET, and KO mice (Figure S2A) exhibit similar surveillance indices *in vivo* including their process extension (Figure S2B), process retractions (Figure S2C), and process velocity (Figure S2D) rates. This is consistent with previous reports.[34,35]

Next, we examined P2RY12 expression in microglia after seizures in basal and post-KA (90 min) in P2RY12-sufficient mice. We selected 90 min because this seemed like the earliest time when differences between microglial- or P2RY12-sufficient versus deficient mice show seizure severity differences (Figures 3A and 3G). Microglia retrained their P2RY12 expression at this time point in both the CA1 region and the somatosensory cortex (Figure S3). To evaluate whether P2RY12 signaling influences microglial structural remodeling during seizure activity, we performed Sholl analyses on microglia in hippocampal CA1 (Figures 4A and 4B) and the somatosensory cortex (Figures 4C and 4D) regions of fixed tissue from WT and gKO littermate mice under basal and post-KA (90 min) conditions. Under basal conditions, WT and gKO microglia were highly ramified with indistinguishable ramification indices in accordance with microglial surveillance function in both the CA1 (Figure 4B) and cortex areas (Figure 4D). Following KA-induced seizures, WT microglia were able to maintain their ramified morphology to a greater extent, whereas there was substantial reduction in process branching in gKO microglia in comparison to WT microglia in both the CA1 (Figure 4B) and cortex (Figure 4D) areas. These results indicate that P2RY12 signaling is critical to the preservation of microglial structural complexity in the context of seizure activity. The reduced ramification in microglia from gKO mice underscores increased microglial de-ramification which might lead to diminished structural engagement with hyperactive circuits and therefore contribute to the increased neuronal activation and seizure severity observed our experiments.

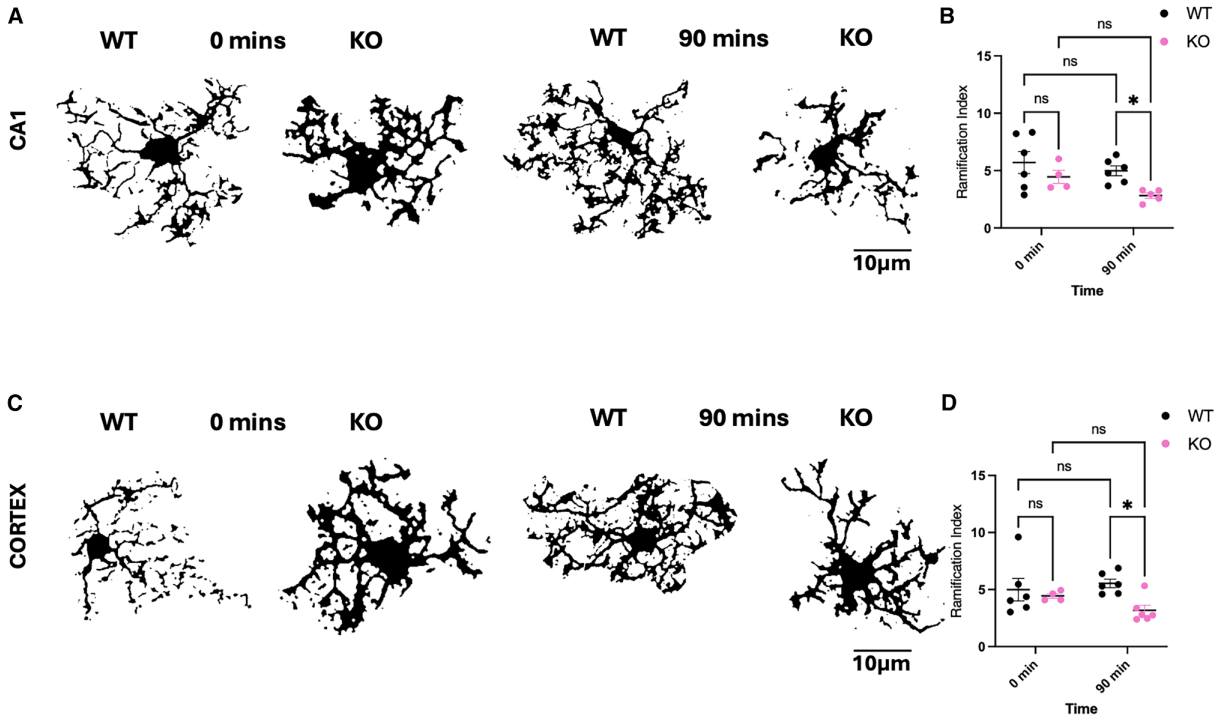

Figure 4. P2RY12 regulates microglial morphological complexity following seizures

(A–D) Representative confocal images (A and C) of IBA1^{+} microglia and quantification of the ramification index (B and D) from hippocampal CA1 (A and B) and the somatosensory cortex (C and D) regions in wild-type (WT) and P2RY12$^{-/-}$ (KO) littermate mice under baseline (0 min) and post-seizure (90 min) conditions following kainic acid administration. Scale bars in (A) and (C) are 10 µm. Data shown as mean ± SEM. *N* = 4–6 mice each. Statistics done by two-way ANOVA with Tukey's post hoc test. *$p < 0.05$.

A P2RY12 deficiency enhances neuronal activation after KA treatment

As indicated earlier, a P2RY12 deficiency leads to increased seizure severity (Figure 3). Therefore, we further investigated if this increased seizure severity was paralleled by any shifts in neuronal activation corresponding to seizure induction. To address this question, we employed cFos immunolabeling, known to indicate neuronal activity, to evaluate the level of seizure-evoked activation in hippocampal CA1 and the somatosensory cortex of WT and gKO mice at basal levels and 90 min of KA treatment. At basal states (0 min), expression of cFos was lower in gKO mice compared to WT mice in both brain regions (Figures 5A–5D). However, 90 min post-KA treatment, the P2RY12 gKO mice showed higher expression of cFos than WT mice in both brain regions, indicating higher neuronal activity in the absence of P2RY12 signaling during seizures (Figures 5A–5D). These data indicate that P2RY12 signaling is involved in controlling seizure-induced neuronal excitation, especially in the hippocampus and cortex. The exaggerated cFos response in P2RY12 KO mice suggests that microglial P2RY12 activity is required to limit excessive neuronal firing during KA-induced hyperexcitability, consistent with the increased seizure severity (Figure 3) and impaired microglial ramification (Figure 4) observed in previous studies.

P2RY12 signaling maintains inhibitory synaptic coverage during seizures

Since loss of P2RY12 signaling led to exaggerated neuronal activation, we next asked whether this hyperexcitability was accompanied by changes in inhibitory synaptic signaling with a P2RY12 deficiency. To test this, we examined expression of the VGAT, a presynaptic marker of inhibitory terminals in both hippocampal CA1 and cortical regions of gKO and WT mice at baseline and 90 min following KA-induced seizures. Under basal conditions, WT mice showed extensive VGAT area coverage in CA1 and cortex, while gKO mice showed reduced VGAT area even in the absence of seizures, indicating an inherent deficiency in neuronal inhibition under basal conditions. Upon seizure induction, the VGAT area was reduced in both the CA1 and cortex in WT mice, with significant reduction detected only in the cortex. However, in gKO mice in both brain regions VGAT expression was almost non-existent at 90 min of KA-treatment (Figures 6A–6C). These findings demonstrate that P2RY12 signaling is critical for maintaining inhibitory synaptic coverage in both the absence and presence of seizure activity. The pronounced reduction in VGAT-positive area in gKO mice indicates that disruption of microglial P2RY12 impairs the preservation of inhibitory terminals in basal and hyperexcited states, providing a potential mechanism for the heightened neuronal activation and seizure severity observed in these mice.

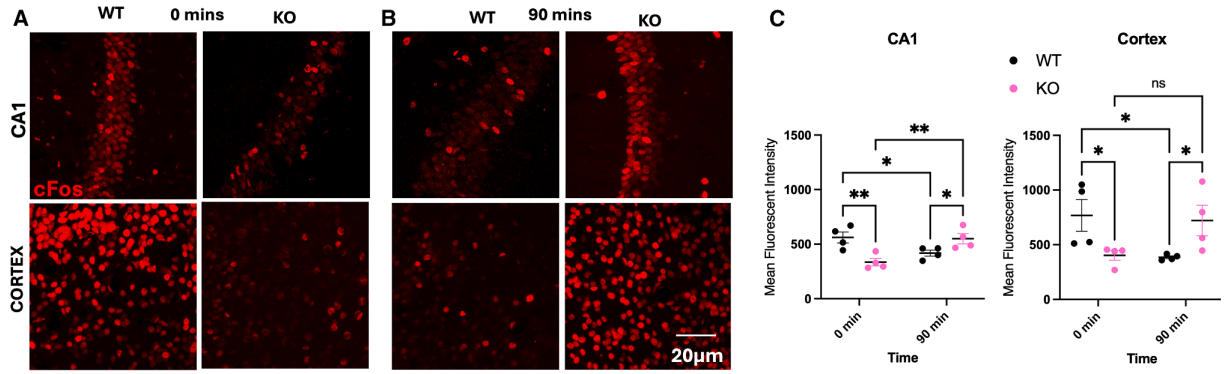

Figure 5. P2RY12 deficiency enhances cFos expression following seizures

(A and B) Representative confocal images of cFos immunoreactivity from the hippocampal CA1 (A) and somatosensory cortex (B) regions in wild-type (WT) and P2RY12$^{-/-}$ (KO) mice under baseline (0 min) and post-seizure (90 min) conditions following kainic acid administration.

(C) Quantification of mean cFos fluorescent intensity in the CA1 (left) and cortex (right) across genotypes and time points. *N* = 4 mice each. Scale bars in (B) are 20 μm. Data shown as mean ± SEM. Statistics by two-way ANOVA with Tukey's post hoc test. *$p < 0.05$; **$p < 0.01$.

DISCUSSION

In the current work, we show that mice with microglial-specific genetically deficient mice show increased seizure severity in response to chemoconvulsive KA-induced seizures (Figure 1) and electrical seizures (Figure 2) consistent with previous results from us and others using pharmacological[15] and pharmacogenetic[13–15] approaches. Together, these results provide overwhelmingly supportive evidence for highlighting a neuroprotective role for microglia in various seizure paradigms. Furthermore, both a global and a microglial-specific P2RY12 deletion provided molecular support for microglial contributions to experimental seizures (Figure 3), again consistent with previous report for neuroprotective microglial contributions to seizures from broad G_i[50] and specific P2RY12[32,41] mechanisms. Additionally, we find that a P2RY12 deficiency impairs microglial abilities to maintain their morphological state following seizures (Figure 4) co-incident with increased neuronal activation states (Figure 5) and reduced inhibitory synaptic density (Figure 6). In summary, this work shows that microglia are integral to the control of hyperexcitability, that P2RY12 signaling is essential to microglia in controlling excitability, and that P2RY12 has implications for microglial morphology, network activation, and inhibitory synapse structure in networks during seizures.

Microglial roles in experimental seizures

Microglial roles in seizure disorders have been hotly debated. Initial ideas at the beginning of the century suggested that because of the known seizure-promoting roles for inflammatory mediators like IL-1β and microglial ability to release such inflammatory molecules, microglia were suggested to perform seizure-promoting functions.[48,49] For example, several studies have shown that following KA-induced seizures, microglia express IL-1β and other pro-inflammatory cytokines.[18–22] These

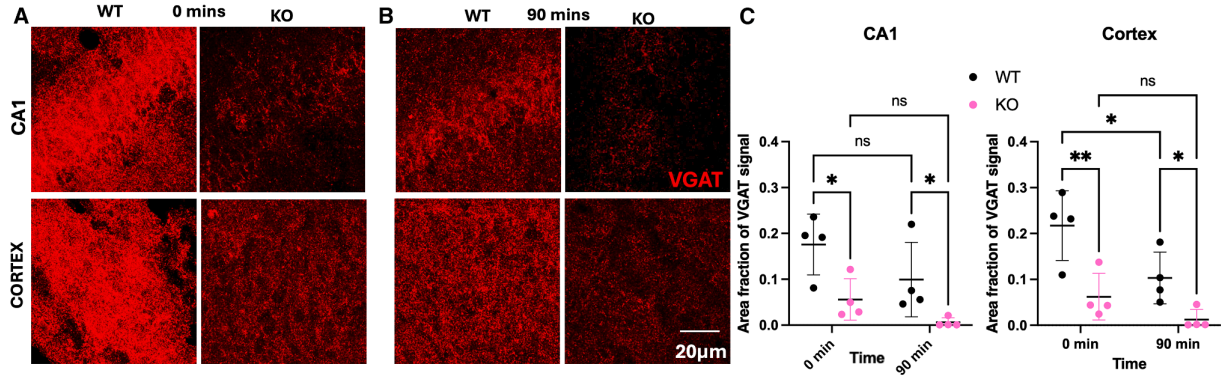

Figure 6. P2RY12 deficiency reduces inhibitory synaptic marker expression following seizures

(A and B) Representative confocal images of VGAT immunoreactivity from the hippocampal CA1 (A) and somatosensory cortex (B) regions in wild-type (WT) and P2RY12$^{-/-}$ (KO) mice under baseline (0 min) and post-seizure (90 min) conditions following kainic acid administration.

(C) Quantification of VGAT-labeled area per μm of tissue section in the CA1 (left) and cortex (right) across genotypes and time points. *N* = 4 mice each. Scale bars in (B) are 20 μm. Data shown as mean ± SEM. Statistics by two-way ANOVA with Tukey's post hoc test. *$p < 0.05$; **$p < 0.01$.

cytokines facilitate neuronal excitability[50–52] and thus would promote seizures in such a context. Therefore, by such considerations, it can be expected that microglial activities in seizure contexts promote seizures. Furthermore, in the developing brain, peak seizure sensitivity occurred at the same time as peak microglial density.[23] Nevertheless, while this association was suggested to be causal, evidence provided was at best correlational and lacked direct causal testing.

More recently, several approaches have been employed to more directly test microglial roles in seizure disorders. In an initial pharmacogenetic microglial ablation approach, microglia were found to be inconsequential to acute seizure phenotypes following chemoconvulsive pilocarpine administration. However, the same study showed that following an inflammatory pre-conditioning with lipopolysaccharide, microglia were neuroprotective to pilocarpine induced seizures.[13] Consistent with this, a different pharmacogenetic approach also showed neuroprotective roles for microglia in chemoconvulsive KA-induced seizures.[14] However, such pharmacogenetic approaches have been shown to themselves elicit neuroinflammation[16] making it difficult to ascertain whether exacerbated seizures with microglial ablation by these methods are a result of losing neuroprotective microglia or having increased neuroinflammation. These concerns raised the need to employ microglial ablation strategies that concomitant inflammation.

In recent years between 2014 and 2019, two such approaches have been developed including a pharmacological approach using the PLX family of drugs to eliminate microglia[39,42] and a genetic approach with the "FIRE" mice.[25] In a previous study, using the PLX approach (i.e. treatment with 660mg/kg PLX3397 in the animal chow), we showed that microglia perform neuroprotective roles in multiple seizure paradigms.[15] These results suggest that the exacerbated phenotypes from pharmacogenetic approaches likely result from microglial absence rather than other confounds such as inflammation. Like these results, experiments conducted in a Dravet syndrome model (a genetic model of seizures) in zebrafish showed that while microglia increase their inflammatory IL-1β expression in this seizure model, their ablation using genetic targeting approaches resulted in increased neuronal activity.

Contrary to these findings, a recent study reported, at least in a PTZ chemoconvulsive model during development, that FIRE mice which lack microglia do not show altered seizure severity.[26] However, that study examined only one chemoconvulsive seizure paradigm in which all mice died suggesting that perhaps the induced seizures were too severe to observe differences. Thus, in the current study we employed the FIRE model in adult chemoconvulsive and electrical seizure paradigms and confirmed that a genetic ablation of microglia exacerbates seizures in these paradigms, which is congruent with the majority of studies investigating microglial roles in experimental acute seizure models.[13–17]

It should be noted that consistent with previous studies, we found that microglia density (Figure 1D) and microglial morphologies (Figure 1F) were similar between FIRE WT and HET mice. Nevertheless, FIRE HET mice did not show animal mortality to KA compared to the few mice that died among FIRE WTs (Figures 1H and 1I). While this was not statistically significant, it may suggest that FIRE HET microglia have some differences from FIRE WT microglia that we have not identified. Future studies beyond the scope of the current work, e.g., exploring the transcriptional profile and examining other salient microglial functions between these cell types will need to be done to explore this possibility. In addition, while we find worse seizure phenotypes in FIRE KO mice following IP KA treatment, we cannot rule out effects from differences in pharmacokinetics of KA delivery to the brain. Nevertheless, this concern is mitigated slightly by the fact that we have a consistent phenotype in a non-pharmacological (i.e., electrical) seizure paradigm (Figure 2).

P2RY12 roles in experimental seizures

Molecular mechanisms by which microglia limit seizure severity remains understudied. In the current study, we investigated roles for the P2RY12 receptor in chemoconvulsive KA-induced seizures. Interest in P2RY12 was generated from prior work showing that it is a predominant receptor through which neurons communicate with microglia especially in hyperactive conditions.[28,32,53,54] Moreover, microglial Gi-signaling dampens neuronal excitability in seizure contexts[55] and P2RY12 is the most highly expressed Gi-coupled receptor in microglia.[27] Furthermore, previous work in a developmental febrile seizure model[41] and an adult D1 agonist-induced seizure model,[56] indicated that microglial P2RY12 mitigate seizure severity. Additionally, we previously showed that a P2RY12 deficiency led to exacerbated KA-induced seizures.[32] However, those studies were not conducted on littermates raising the possibility that genetic differences broadly rather than a P2RY12-specific deficiency could account for the aggravated seizure phenotypes in P2RY12 KO mice. Therefore, to more conclusively explore P2RY12 roles in KA-induced seizures, we examined seizures in littermate mice and confirm more severe seizures in littermates lacking P2RY12. Furthermore, with the development of P2RY12 flox mice,[37] we were able to assess microglial-specific contributions and confirmed the results with global KO mice that microglia's role is to limit seizure severity.

In addition, an examination of microglial phenotypes revealed an accelerated de-ramification of microglia in P2RY12 KO microglia following KA treatment. Since microglial ramified processes facilitate their tissue surveillance,[46,47] which regulates microglial physical interactions with neurons such as synapses,[57–59] these results suggest that an increased de-ramification would result in reduced microglial surveillance as well as microglial-neuronal interactions during seizures consistent with previous results.[32,55] These changes in microglia correlated with increased broad neuronal activity and reduced GABAergic inhibitory tone suggesting that microglial process dynamics under P2RY12 control regulates neuronal hyperactivity during seizures.

Future direction

Our results raise additional question for further investigation. For example, while we find reduced cFos in naive KO compared to WT brains (Figure 5), we also find reduced VGAT (suggesting that a reduced inhibitory tone is present) in KO compared to WT brains (Figure 6) which is superficially inconsistent but suggest a need for more detailed functional assessments of these findings. For example, different specific subtypes of neurons

(excitatory v. inhibitory) have not been identified to explain the reduced cFos expression in Figure 5. Moreover, downstream mechanisms of P2RY12 regulation of neuronal phenotypes remain to be determined and should be a focus of subsequent work. In addition, our results warrant further assessment of inhibitory tone such as an assessment of postsynaptic inhibitory markers. Furthermore, the current studies have only investigated P2RY12 contributions to acute seizure phenotypes leaving open roles for the receptor's function in epileptogenic processes that can be a focus of future work as well. Nevertheless, our studies herein firmly implicate microglia and its P2RY12 receptors in the regulation of seizure severity during acute seizures warranting future studies.

Limitations of the study

While informative, our study has some limitations. First, in its exclusive use of genetic approaches to target microglia and P2RY12, our findings cannot rule out developmental effects of these genetic manipulations. Our prior work with pharmacological depletion of microglia using PLX3397[15] show congruent results with the current findings and can mitigate some of this limitation. Nevertheless, future studies should employ an adult-inducible deletion of P2RY12 to further distinguish developmental and functional roles of P2RY12 in seizure severity. Second, the use of genetic approaches as done in the current study has less translational value for patients with seizure disorders. Therefore, more pharmacologically directed approaches would be useful. Moreover, our exclusive use of loss-of-function approaches that exacerbate seizures while elucidating underlying cellular and molecular players in experimental seizure paradigms has less translational values than gain-of-function approaches Therefore, future studies will also have to explore this possibility. Finally, our study lacks detailed examination of neuronal cell-type specific states and physiological function under microglial and P2RY12 control that should be interrogated for a deeper mechanistic understanding of microglial contributions to seizure disorders.

RESOURCE AVAILABILITY

Lead contact

Requests for further information and resources should be directed to and will be fulfilled by the lead contact, Ukpong B. Eyo (ube9q@virginia.edu).

Materials availability

This study did not generate new unique reagents. All commercially available materials used in this study are listed in the key resources table.

Data and code availability

Data

Data reported in this paper will be shared by the lead contact upon request.

Code

This paper does not report original code.

Additional resources

Any additional information required to reanalyze the data reported in this paper is available from the lead contact upon request.

ACKNOWLEDGMENTS

We thank members of the Eyo Lab, the Center for Brain Immunology and Glia (BIG), and the UVA Neuroscience and Pharmacology Departments for valuable input in the development of the project. This study received support from The National Institute of Health, NS119243 (U.B.E.) NS112549 (E.P.-R.), HL007284 (L.E.F.), 5T32GM148379 (S.G.-S.), Gilliam award from the HHMI (S.G.-S.), and the Owens Family Foundation (U.B.E.).

AUTHOR CONTRIBUTIONS

Conceptualization, S.G.-S. and U.B.E.; methodology, S.G.-S., L.E.F., E.P.-R., and U.B.E.; investigation, L.E.F., S.G.-S., M.D., A.O.L.-O., A.D., W.A.M. III, R.P.G., K.S., A.N., and S.C.; writing – original draft, S.G.-S., E.P.-R., and U.B.E.; Writing—review and editing, L.E.F., and U.B.E.; funding, S.G.-S., E.P.-R., and U.B.E.; supervision, U.B.E.

DECLARATION OF INTERESTS

The authors declare no competing interests.

STAR★METHODS

Detailed methods are provided in the online version of this paper and include the following:

- KEY RESOURCES TABLE
- EXPERIMENTAL MODEL AND STUDY PARTICIPANT DETAILS
  - Animals
  - Sex as a biological variable
- METHOD DETAILS
  - Chemoconvulsive seizure induction
  - Animal surgeries
  - Kindling protocol
  - Immunohistochemistry and confocal microscopy
  - *In vivo* multiphoton imaging
- QUANTIFICATION AND STATISTICAL ANALYSIS
  - Sholl analysis of microglial morphology for ramification index
  - Statistical analysis

SUPPLEMENTAL INFORMATION

Supplemental information can be found online at https://doi.org/10.1016/j.isci.2026.116563.

Received: January 13, 2026
Revised: March 8, 2026
Accepted: June 9, 2026
Published: July 2, 2026

REFERENCES

1. Sepeta, L.N., Berl, M.M., and Gaillard, W.D. (2018). Imaging episodic memory during development and childhood epilepsy. J. Neurodev. Disord. *10*, 40. https://doi.org/10.1186/s11689-018-9255-8.
2. Hesdorffer, D.C., Logroscino, G., Benn, E.K.T., Katri, N., Cascino, G., and Hauser, W.A. (2011). Estimating risk for developing epilepsy: a population-based study in Rochester, Minnesota. Neurology *76*, 23–27. https://doi.org/10.1212/WNL.0b013e318204a36a.
3. Streng, M.L., Froula, J.M., and Krook-Magnuson, E. (2023). The cerebellum's understated role and influences in the epilepsies. Neurobiol. Dis. *183*, 106160. https://doi.org/10.1016/j.nbd.2023.106160.
4. Löscher, W., Potschka, H., Sisodiya, S.M., and Vezzani, A. (2020). Drug Resistance in Epilepsy: Clinical Impact, Potential Mechanisms, and New Innovative Treatment Options. Pharmacol. Rev. *72*, 606–638. https://doi.org/10.1124/pr.120.019539.
5. Pong, A.W., Xu, K.J., and Klein, P. (2023). Recent advances in pharmacotherapy for epilepsy. Curr. Opin. Neurol. *36*, 77–85. https://doi.org/10.1097/WCO.0000000000001144.

6. Gonzalez-Giraldo, E., and Sullivan, J.E. (2020). Advances in the Treatment of Drug-Resistant Pediatric Epilepsy. Semin. Neurol. *40*, 257–262. https://doi.org/10.1055/s-0040-1702941.

7. Patel, D.C., Tewari, B.P., Chaunsali, L., and Sontheimer, H. (2019). Neuron-glia interactions in the pathophysiology of epilepsy. Nat. Rev. Neurosci. *20*, 282–297. https://doi.org/10.1038/s41583-019-0126-4.

8. Chen, P., Chen, F., and Zhou, B. (2022). Understanding the Role of Glia-Neuron Communication in the Pathophysiology of Epilepsy: A Review. J. Integr. Neurosci. *21*, 102. https://doi.org/10.31083/j.jin2104102.

9. Ghouli, M.R., and Binder, D.K. (2025). Neuroglia in epilepsy. Handb. Clin. Neurol. *210*, 69–86. https://doi.org/10.1016/B978-0-443-19102-2.00016-8.

10. Foiadelli, T., Santangelo, A., Costagliola, G., Costa, E., Scacciati, M., Riva, A., Volpedo, G., Smaldone, M., Bonuccelli, A., Clemente, A.M., et al. (2023). Neuroinflammation and status epilepticus: a narrative review unraveling a complex interplay. Front. Pediatr. *11*, 1251914. https://doi.org/10.3389/fped.2023.1251914.

11. Henshall, D.C., and Engel, T. (2015). P2X purinoceptors as a link between hyperexcitability and neuroinflammation in status epilepticus. Epilepsy Behav. *49*, 8–12. https://doi.org/10.1016/j.yebeh.2015.02.031.

12. Vezzani, A., Di Sapia, R., Kebede, V., Balosso, S., and Ravizza, T. (2023). Neuroimmunology of status epilepticus. Epilepsy Behav. *140*, 109095. https://doi.org/10.1016/j.yebeh.2023.109095.

13. Mirrione, M.M., Konomos, D.K., Gravanis, I., Dewey, S.L., Aguzzi, A., Heppner, F.L., and Tsirka, S.E. (2010). Microglial ablation and lipopolysaccharide preconditioning affects pilocarpine-induced seizures in mice. Neurobiol. Dis. *39*, 85–97. https://doi.org/10.1016/j.nbd.2010.04.001.

14. Wu, W., Li, Y., Wei, Y., Bosco, D.B., Xie, M., Zhao, M.G., Richardson, J.R., and Wu, L.J. (2020). Microglial depletion aggravates the severity of acute and chronic seizures in mice. Brain Behav. Immun. *89*, 245–255. https://doi.org/10.1016/j.bbi.2020.06.028.

15. Gibbs-Shelton, S., Benderoth, J., Gaykema, R.P., Straub, J., Okojie, K.A., Uweru, J.O., Lentferink, D.H., Rajbanshi, B., Cowan, M.N., Patel, B., et al. (2023). Microglia play beneficial roles in multiple experimental seizure models. Glia *71*, 1699–1714. https://doi.org/10.1002/glia.24364.

16. Bruttger, J., Karram, K., Wörtge, S., Regen, T., Marini, F., Hoppmann, N., Klein, M., Blank, T., Yona, S., Wolf, Y., et al. (2015). Genetic Cell Ablation Reveals Clusters of Local Self-Renewing Microglia in the Mammalian Central Nervous System. Immunity *43*, 92–106. https://doi.org/10.1016/j.immuni.2015.06.012.

17. Brenet, A., Somkhit, J., Csaba, Z., Ciura, S., Kabashi, E., Yanicostas, C., and Soussi-Yanicostas, N. (2024). Microglia Mitigate Neuronal Activation in a Zebrafish Model of Dravet Syndrome. Cells *13*, 684. https://doi.org/10.3390/cells13080684.

18. Vezzani, A., Conti, M., De Luigi, A., Ravizza, T., Moneta, D., Marchesi, F., and De Simoni, M.G. (1999). Interleukin-1beta immunoreactivity and microglia are enhanced in the rat hippocampus by focal kainate application: functional evidence for enhancement of electrographic seizures. J. Neurosci. *19*, 5054–5065. https://doi.org/10.1523/JNEUROSCI.19-12-05054.1999.

19. Eriksson, C., Tehranian, R., Iverfeldt, K., Winblad, B., and Schultzberg, M. (2000). Increased expression of mRNA encoding interleukin-1beta and caspase-1, and the secreted isoform of interleukin-1 receptor antagonist in the rat brain following systemic kainic acid administration. J. Neurosci. Res. *60*, 266–279. https://doi.org/10.1002/(SICI)1097-4547(20000415)60:2<266::AID-JNR16>3.0.CO;2.

20. Rizzi, M., Perego, C., Aliprandi, M., Richichi, C., Ravizza, T., Colella, D., Velíšková, J., Moshé, S.L., De Simoni, M.G., and Vezzani, A. (2003). Glia activation and cytokine increase in rat hippocampus by kainic acid-induced status epilepticus during postnatal development. Neurobiol. Dis. *14*, 494–503. https://doi.org/10.1016/j.nbd.2003.08.001.

21. Zheng, H., Zhu, W., Zhao, H., Wang, X., Wang, W., and Li, Z. (2010). Kainic acid-activated microglia mediate increased excitability of rat hippocampal neurons in vitro and in vivo: crucial role of interleukin-1beta. Neuroimmunomodulation *17*, 31–38. https://doi.org/10.1159/000243083.

22. Avignone, E., Ulmann, L., Levavasseur, F., Rassendren, F., and Audinat, E. (2008). Status epilepticus induces a particular microglial activation state characterized by enhanced purinergic signaling. J. Neurosci. *28*, 9133–9144. https://doi.org/10.1523/JNEUROSCI.1820-08.2008.

23. Kim, I., Mlsna, L.M., Yoon, S., Le, B., Yu, S., Xu, D., and Koh, S. (2015). A postnatal peak in microglial development in the mouse hippocampus is correlated with heightened sensitivity to seizure triggers. Brain Behav. *5*, e00403. https://doi.org/10.1002/brb3.403.

24. Mo, M., Eyo, U.B., Xie, M., Peng, J., Bosco, D.B., Umpierre, A.D., Zhu, X., Tian, D.S., Xu, P., and Wu, L.J. (2019). Microglial P2Y12 Receptor Regulates Seizure-Induced Neurogenesis and Immature Neuronal Projections. J. Neurosci. *39*, 9453–9464. https://doi.org/10.1523/JNEUROSCI.0487-19.2019.

25. Rojo, R., Raper, A., Ozdemir, D.D., Lefevre, L., Grabert, K., Wollscheid-Lengeling, E., Bradford, B., Caruso, M., Gazova, I., Sánchez, A., et al. (2019). Deletion of a Csf1r enhancer selectively impacts CSF1R expression and development of tissue macrophage populations. Nat. Commun. *10*, 3215. https://doi.org/10.1038/s41467-019-11053-8.

26. O'Keeffe, M., Booker, S.A., Walsh, D., Li, M., Henley, C., Simões de Oliveira, L., Liu, M., Wang, X., Banqueri, M., Ridley, K., et al. (2025). Typical development of synaptic and neuronal properties can proceed without microglia in the cortex and thalamus. Nat. Neurosci. *28*, 268–279. https://doi.org/10.1038/s41593-024-01833-x.

27. Hickman, S.E., Kingery, N.D., Ohsumi, T.K., Borowsky, M.L., Wang, L.c., Means, T.K., and El Khoury, J. (2013). The microglial sensome revealed by direct RNA sequencing. Nat. Neurosci. *16*, 1896–1905.

28. Cserép, C., Pósfai, B., and Dénes, Á. (2021). Shaping Neuronal Fate: Functional Heterogeneity of Direct Microglia-Neuron Interactions. Neuron *109*, 222–240. https://doi.org/10.1016/j.neuron.2020.11.007.

29. Cserép, C., Pósfai, B., Lénárt, N., Fekete, R., László, Z.I., Lele, Z., Orsolits, B., Molnár, G., Heindl, S., Schwarcz, A.D., et al. (2020). Microglia monitor and protect neuronal function through specialized somatic purinergic junctions. Science *367*, 528–537. https://doi.org/10.1126/science.aax6752.

30. Eyo, U.B., Gu, N., De, S., Dong, H., Richardson, J.R., and Wu, L.J. (2015). Modulation of microglial process convergence toward neuronal dendrites by extracellular calcium. J. Neurosci. *35*, 2417–2422. https://doi.org/10.1523/JNEUROSCI.3279-14.2015.

31. Eyo, U.B., Murugan, M., and Wu, L.J. (2017). Microglia-Neuron Communication in Epilepsy. Glia *65*, 5–18. https://doi.org/10.1002/glia.23006.

32. Eyo, U.B., Peng, J., Swiatkowski, P., Mukherjee, A., Bispo, A., and Wu, L.J. (2014). Neuronal hyperactivity recruits microglial processes via neuronal NMDA receptors and microglial P2Y12 receptors after status epilepticus. J. Neurosci. *34*, 10528–10540.

33. Gu, N., Eyo, U.B., Murugan, M., Peng, J., Matta, S., Dong, H., and Wu, L.J. (2016). Microglial P2Y12 receptors regulate microglial activation and surveillance during neuropathic pain. Brain Behav. Immun. *55*, 82–92. https://doi.org/10.1016/j.bbi.2015.11.007.

34. Haynes, S.E., Hollopeter, G., Yang, G., Kurpius, D., Dailey, M.E., Gan, W.B., and Julius, D. (2006). The P2Y12 receptor regulates microglial activation by extracellular nucleotides. Nat. Neurosci. *9*, 1512–1519. https://doi.org/10.1038/nn1805.

35. Sipe, G.O., Lowery, R.L., Tremblay, M.È., Kelly, E.A., Lamantia, C.E., and Majewska, A.K. (2016). Microglial P2Y12 is necessary for synaptic plasticity in mouse visual cortex. Nat. Commun. *7*, 10905. https://doi.org/10.1038/ncomms10905.

36. Bollinger, J.L., Dadosky, D.T., Flurer, J.K., Rainer, I.L., Woodburn, S.C., and Wohleb, E.S. (2023). Microglial P2Y12 mediates chronic stress-induced synapse loss in the prefrontal cortex and associated behavioral consequences. Neuropsychopharmacology *48*, 1347–1357. https://doi.org/10.1038/s41386-022-01519-7.

37. Peng, J., Liu, Y., Umpierre, A.D., Xie, M., Tian, D.S., Richardson, J.R., and Wu, L.J. (2019). Microglial P2Y12 receptor regulates ventral hippocampal CA1 neuronal excitability and innate fear in mice. Mol. Brain *12*, 71. https://doi.org/10.1186/s13041-019-0492-x.

38. Yei, J., Lee, N.K., Ryu, S., Ryu, S.E., Lee, J., Park, T., Jeong, Y., Kang, R., Kwon, H.K., Kim, S.G., et al. (2025). Glioma-Associated Microglia Potentiate Neuronal Hyper-Excitability in the Glioma Environment. Neuro Oncol. *27*, 3058–3071. https://doi.org/10.1093/neuonc/noaf181.

39. Green, K.N., Crapser, J.D., and Hohsfield, L.A. (2020). To Kill a Microglia: A Case for CSF1R Inhibitors. Trends Immunol. *41*, 771–784. https://doi.org/10.1016/j.it.2020.07.001.

40. Claeys, W., Verhaege, D., Van Imschoot, G., Van Wonterghem, E., Van Acker, L., Amelinck, L., De Ponti, F.F., Scott, C., Geerts, A., Van Steenkiste, C., et al. (2023). Limitations of PLX3397 as a microglial investigational tool: peripheral and off-target effects dictate the response to inflammation. Front. Immunol. *14*, 1283711. https://doi.org/10.3389/fimmu.2023.1283711.

41. Wan, Y., Feng, B., You, Y., Yu, J., Xu, C., Dai, H., Trapp, B.D., Shi, P., Chen, Z., and Hu, W. (2020). Microglial Displacement of GABAergic Synapses Is a Protective Event during Complex Febrile Seizures. Cell Rep. *33*, 108346. https://doi.org/10.1016/j.celrep.2020.108346.

42. Elmore, M.R.P., Najafi, A.R., Koike, M.A., Dagher, N.N., Spangenberg, E.E., Rice, R.A., Kitazawa, M., Matusow, B., Nguyen, H., West, B.L., and Green, K.N. (2014). Colony-stimulating factor 1 receptor signaling is necessary for microglia viability, unmasking a microglia progenitor cell in the adult brain. Neuron *82*, 380–397. https://doi.org/10.1016/j.neuron.2014.02.040.

43. Okojie, A.K., Uweru, J.O., Coburn, M.A., Li, S., Cao-Dao, V.D., and Eyo, U.B. (2023). Distinguishing the effects of systemic CSF1R inhibition by PLX3397 on microglia and peripheral immune cells. J. Neuroinflammation *20*, 242. https://doi.org/10.1186/s12974-023-02924-5.

44. Straub, J., Gawda, A., Ravichandran, P., McGrew, B., Nylund, E., Kang, J., Burke, C., Vitko, I., Scott, M., Williamson, J., et al. (2020). Characterization of kindled VGAT-Cre mice as a new animal model of temporal lobe epilepsy. Epilepsia *61*, 2277–2288. https://doi.org/10.1111/epi.16651.

45. Gachet, C. (2012). P2Y(12) receptors in platelets and other hematopoietic and non-hematopoietic cells. Purinergic Signal. *8*, 609–619. https://doi.org/10.1007/s11302-012-9303-x.

46. Davalos, D., Grutzendler, J., Yang, G., Kim, J.V., Zuo, Y., Jung, S., Littman, D.R., Dustin, M.L., and Gan, W.B. (2005). ATP mediates rapid microglial response to local brain injury in vivo. Nat. Neurosci. *8*, 752–758. https://doi.org/10.1038/nn1472.

47. Nimmerjahn, A., Kirchhoff, F., and Helmchen, F. (2005). Resting microglial cells are highly dynamic surveillants of brain parenchyma in vivo. Science *308*, 1314–1318. https://doi.org/10.1126/science.1110647.

48. Devinsky, O., Vezzani, A., Najjar, S., De Lanerolle, N.C., and Rogawski, M.A. (2013). Glia and epilepsy: excitability and inflammation. Trends Neurosci. *36*, 174–184. https://doi.org/10.1016/j.tins.2012.11.008.

49. Vezzani, A., Auvin, S., Ravizza, T., and Aronica, E. (2012). In Jasper's Basic Mechanisms of the Epilepsies, J.L. Noebels, M. Avoli, M.A. Rogawski, R.W. Olsen, and A.V. Delgado-Escueta, eds. (Oxford University Press, USA).

50. Schäfers, M., and Sorkin, L. (2008). Effect of cytokines on neuronal excitability. Neurosci. Lett. *437*, 188–193. https://doi.org/10.1016/j.neulet.2008.03.052.

51. Vezzani, A., and Viviani, B. (2015). Neuromodulatory properties of inflammatory cytokines and their impact on neuronal excitability. Neuropharmacology *96*, 70–82. https://doi.org/10.1016/j.neuropharm.2014.10.027.

52. Galic, M.A., Riazi, K., and Pittman, Q.J. (2012). Cytokines and brain excitability. Front. Neuroendocrinol. *33*, 116–125. https://doi.org/10.1016/j.yfrne.2011.12.002.

53. Dissing-Olesen, L., LeDue, J.M., Rungta, R.L., Hefendehl, J.K., Choi, H.B., and MacVicar, B.A. (2014). Activation of neuronal NMDA receptors triggers transient ATP-mediated microglial process outgrowth. J. Neurosci. *34*, 10511–10527. https://doi.org/10.1523/JNEUROSCI.0405-14.2014.

54. Uweru, J.O., and Eyo, U.B. (2019). A decade of diverse microglial-neuronal physical interactions in the brain (2008-2018). Neurosci. Lett. *698*, 33–38. https://doi.org/10.1016/j.neulet.2019.01.001.

55. Merlini, M., Rafalski, V.A., Ma, K., Kim, K.Y., Bushong, E.A., Rios Coronado, P.E., Yan, Z., Mendiola, A.S., Sozmen, E.G., Ryu, J.K., et al. (2021). Microglial Gi-dependent dynamics regulate brain network hyperexcitability. Nat. Neurosci. *24*, 19–23. https://doi.org/10.1038/s41593-020-00756-7.

56. Badimon, A., Strasburger, H.J., Ayata, P., Chen, X., Nair, A., Ikegami, A., Hwang, P., Chan, A.T., Graves, S.M., Uweru, J.O., et al. (2020). Negative feedback control of neuronal activity by microglia. Nature *586*, 417–423.

57. Wake, H., Moorhouse, A.J., Jinno, S., Kohsaka, S., and Nabekura, J. (2009). Resting microglia directly monitor the functional state of synapses in vivo and determine the fate of ischemic terminals. J. Neurosci. *29*, 3974–3980. https://doi.org/10.1523/JNEUROSCI.4363-08.2009.

58. Tremblay, M.È., Stevens, B., Sierra, A., Wake, H., Bessis, A., and Nimmerjahn, A. (2011). The role of microglia in the healthy brain. J. Neurosci. *31*, 16064–16069. https://doi.org/10.1523/jneurosci.4158-11.2011.

59. Tremblay, M.È., Lowery, R.L., and Majewska, A.K. (2010). Microglial interactions with synapses are modulated by visual experience. PLoS Biol. *8*, e1000527. https://doi.org/10.1371/journal.pbio.1000527.

60. Racine, R.J. (1972). Modification of seizure activity by electrical stimulation. II. Motor seizure. Electroencephalogr. Clin. Neurophysiol. *32*, 281–294. https://doi.org/10.1016/0013-4694(72)90177-0.

STAR★METHODS

KEY RESOURCES TABLE

REAGENT or RESOURCE	SOURCE	IDENTIFIER
Antibodies		
Rabbit anti-Iba1	FUJIFILM Wako Pure Chemical Corporation	Cat #019-19741; RRID AB_839504
Rabbit anti-cFos	Synaptic Systems	Cat #226008; RRID AB_2891278
Rabbit anti-VGAT	Synaptic Systems	Cat #131004; RRID AB_887873
5% normal donkey serum	Jackson ImmunoResearch Laboratories Inc.	Cat #017-000-121; RRID AB_2337258
Phosphate Buffered Saline (PBS)	Sigma Aldrich	Cat #P3813-10PAK; RRID AB_258116
Donkey anti-guinea pig IgG Alexa Fluor 647	Jackson ImmunoResearch Laboratories Inc.	Cat #706-605-148; RRID AB_234046
Donkey anti-rabbit IgG Alexa Fluor 488	ThermoFisher Scientific	Cat #A-21206
Goat anti-rabbit IgG Alexa Fluor 488	ThermoFisher Scientific	Cat #A-11034
Goat anti-rat 647 IgG Alexa Fluor 647	ThermoFisher Scientific	Cat #A-21247
Goat anti-rat 680 IgG Alexa Fluor 680	ThermoFisher Scientific	Cat #A21096
Donkey anti-rat IgG Alexa Fluor 647	Jackson ImmunoResearch Laboratories Inc.	Cat #712-605-153; RRID AB_2340694
Donkey anti-rabbit IgG Alexa Fluor 594	ThermoFisher Scientific	Cat #R37119
donkey anti-rabbit IgG Alexa Fluor 647	ThermoFisher Scientific	Cat #A-31573
goat anti-mouse 647 IgG Alexa Fluor 647	ThermoFisher Scientific	Cat #A32728
goat anti-mouse IgG Alexa Fluor 488	ThermoFisher Scientific	Cat #A-11001
NucBlue	ThermoFisher Scientific	Cat #R37605
Hoechst 33342	ThermoFisher Scientific	Cat #H3570
Experimental models: Organisms/strains		
C57BL/6J	Jackson Laboratories	#000664
CX3CR1-GFP	Jackson Laboratories	#005582
P2RY12KO	Eyo Lab, University of Virginia	N/A
CX3CR1^{Cre}	Jackson Laboratories	#025524
P2RY12 $^{fl/fl}$	Dr. Long-Jun Wu, University of Texas Health in Houston	N/A
Csf1r$^{\Delta FIRE/\Delta FIRE}$	Jackson Laboratories	#32783
Software and algorithms		
ImageJ	NIH	https://imagej.net/ij/
Prism GraphPad	GraphPad Software	https://www.graphpad.com
TWin	Grass Technologies, Astro-Med Inc.	https://www.astronovainc.com

EXPERIMENTAL MODEL AND STUDY PARTICIPANT DETAILS

Animals

All animal experiments were carried out according to guidelines and regulations of the University of Virginia's Institutional Animal Care and Use Committee with protocol number 4237. Animals were housed under controlled temperature, humidity, and light (12:12 h light: dark cycle), with food and water available *ad libitum*. Both male and female mice on a C57BL/6J background between 2 and 4 months of age were used, and consisted of: C57BL/6J mice as wildtype mice; CX3CR1$^{GFP/+}$ expressing GFP under control of the fractalkine receptor (CX3CR1) promoter (Jackson Lab, #005582); P2RY12 KO mice; CX3CR1^{Cre} mice (Jackson Lab, #025524); P2RY12 $^{fl/fl}$ mice as a generous gift from Dr. Long-Jun Wu at the University of Texas Health in Houston; *Csf1r*$^{\Delta FIRE/\Delta FIRE}$ as a generous gift from Dr. Sandro da Mesquita, Mayo Clinic and maintained on a mixed CBA and C57BL/6J background. Mice were housed in groups for the experiment without special environmental enrichment.

Sex as a biological variable

Both sexes were included in this study. Data were not presented separated by sex because sex differences were not observed in the initial analysis.

METHOD DETAILS

Chemoconvulsive seizure induction

For chemoconvulsive seizure initiation model, 2-4-month-old mice were used, and i.p. injected with kainic acid (KA) at 24 mg/kg body weight which is a dose we have previously established for use to effectively induce seizures with limited mortality in our lab.[15] Control mice were injected with equal volumes of saline that was used as the vehicle to dissolve the kainic acid. Seizures were scored using a modified Racine scale as follows: (1) freezing behavior; (2) rigid posture with raised tail; (3) continuous head bobbing and forepaws shaking; (4) rearing, falling, and jumping; (5) continuous occurrence of level 4; (6) loss of posture and generalized convulsion activity and (7) for death.[22,32,60] Scores were recorded every 5 min for up to 3 h and given based on the summary of the mouse behavior over the 5-min interval. The experimenter was ''blind'' to the prior condition of the mice. The seizure scores are presented as the median of the scores and the area under the curve was analyzed. For pharmacological depletion, mice were treated with PLX3397 (660 mg/kg) for 7 days prior to KA treatment.

Animal surgeries

Surgeries were performed on 8-week-old mice under isoflurane anesthesia. A Kopf stereotaxic apparatus was used to guide implantation of an EEG recording headset that included a bipolar Teflon-coated stainless-steel stimulating electrode (A-M Systems, diameter = 0.008″, #791400), bilateral supradural cortical electrodes, and a cerebellar reference electrode. Electrodes were connected to a six-pin pedestal (Plastics One), which was secured to the skull with dental cement. The depth electrode was placed in the left hippocampus, targeting the perforant path at 3 mm posterior, 3 mm lateral, and 3 mm depth to bregma. Animal discomfort was minimized with bupivacaine and ketoprofen (4 mg/kg delivered subcutaneously after surgery and every 24 h as needed). All studies were performed in accordance with protocols approved by the Animal Care and Use Committee of the University of Virginia and ARRIVE guidelines.

Kindling protocol

After at least 1 week for recovery from surgery, mice were connected to a video-EEG monitoring system (AURA LTM64 using TWin software, Grass) via a flexible cable and commutator (Plastics One). One day later, we measured the afterdischarge threshold (ADT); the hippocampal electrode was connected to a constant current stimulator (A-M Systems, Model 2100), and then a 1-millisecond biphasic square wave pulse at 50 Hz was applied for 2 s. The current was initially set at 20 μA and increased in 20 μA increments until an electrographic discharge was observed (2 min between stimulations). The mean ADT was 108 μA (range 40–400). For kindling, the current intensity was set to 1.5× the magnitude of ADT for that mouse and was delivered twice per day, every 48h, with an interval between stimulations of at least 4h. Animals were considered fully kindled when stimulations evoked five consecutive seizures with a behavioral score of at least 5 (bilateral clonus with loss of posture control) on a modified Racine scale. Animals were monitored by continuous video-EEG throughout the experiment (24 h/d, 7 days/wk). EEG data were digitized at 400 Hz, then stored with video for subsequent analysis. Spontaneous seizures were defined as evolving spike-wave discharges with >2-Hz frequency and 3 × the baseline amplitude lasting 15 s or longer. During analysis, electrographic seizures were confirmed by the corresponding video and a behavioral score was assigned.

Immunohistochemistry and confocal microscopy

Mice were perfused with 1x PBS (Life Technologies Corporation, NY, USA) + Heparin 0.05% prior to brain harvesting and post-fixation in 4% PFA for 24h, with the exception of brains used for c-Fos staining, which were only post-fixed in 4% PFA for 1-2h. Brains were then washed in PBS and placed in 15% sucrose solution at 4°C for 24h, then transferred to 30% sucrose solution at 4°C for 24h. Brains were cryopreserved in optimal cutting temperature (OCT) media (Product #: 72592; Electron Microscopy Science, USA) and sectioned into 40-μm-thick free-floating sections obtained by sectioning brains with a cryostat (Model CM1950, Leica). Four sections per mouse were incubated in blocking buffer consisting of 1% Bovine Serum Albumin (BSA, Sigma-Aldrich, Germany, 5% normal donkey serum (Product # 017-000-121; Jackson ImmunoResearch Laboratories Inc. USA) and 0.3% Triton X-100 solution (Product #: 93443; Sigma-Aldrich) in 1x PBS for 1 h at room temperature. Sections were then immersed in primary antibody and blocking buffer solution and placed on a shaker overnight at 4°C.

Primary antibodies used were as follows: rabbit anti-Iba1 (1:500; Cat #019–19741; FUJIFILM Wako Pure Chemical Corporation), rabbit anti-cFos (1:1000; Cat #226008; Synaptic Systems), rabbit anti-VGAT (1:1000; Cat #131004; Synaptic Systems). All secondary antibodies were used at 1:500 dilution and incubated in 1x PBS, 5% normal donkey serum, and secondary antibodies for 2h in the dark. Secondary antibodies used include the following: donkey anti-guinea pig IgG Alexa Fluor 647 (Cat #706-605-148; Jackson ImmunoResearch Laboratories Inc.), donkey anti-rabbit IgG Alexa Fluor 488 (Cat #A-21206; ThermoFisher Scientific), goat anti-rabbit IgG Alexa Fluor 488 (Cat #A-11034; ThermoFisher Scientific), goat anti-rat 647 IgG Alexa Fluor 647 (Cat #A-21247; ThermoFisher Scientific), goat anti-rat 680 IgG Alexa Fluor 680 (Cat #A21096; ThermoFisher Scientific), donkey anti-rat IgG Alexa Fluor 647 (Cat #712-605-153; Jackson ImmunoResearch Laboratories Inc.), donkey anti-rabbit IgG Alexa Fluor 594 (Cat #R37119; ThermoFisher Scientific), donkey anti-rabbit IgG Alexa Fluor 647 (Cat #A-31573; ThermoFisher Scientific), goat anti-mouse 647 IgG Alexa Fluor 647 (Cat #A32728; ThermoFisher Scientific), and goat anti-mouse IgG Alexa Fluor 488 (Cat #A-11001, ThermoFisher Scientific).

Cell nuclei were stained by incubating sections in NucBlue (1 drop per 1 mL of 1x PBS; Hoechst 33342; ThermoFisher Scientific). Slides were imaged on a Stellaris 5 confocal microscope (Leica Microsystems, USA) with 20x, 40x, and 63x objectives.

In vivo multiphoton imaging

To perform cranial window surgery, induction of surgical plane anesthesia with 2–5% isoflurane was first established. Pre-operative analgesics (Bupivacaine) were then administered subcutaneously at the site of incision prior to surgery. Hair and skin of the skull were then removed, and a 3 mm craniectomy 2 mm posterior and 1.5 mm lateral to bregma performed on one hemisphere on the somatosensory cortex. Dura was then removed, followed by the placement of a 3 mm circular No. 1 cover glass (Warner Instruments CS-3R, Cat #: 64–0720). A light-curing dental cement (Tetric EvoFlow) was applied and cured with a Kerr Demi Ultra LED Curing Light (DentalHealth Products). iBond Total Etch glue (Heraeus) was applied to the rest of the skull, except for the region with the window. This was also cured with the LED Curing Light. The light-curing dental glue was used to attach a custom-made head bar onto the other side of the skull from which the craniotomy was performed. Mice were allowed to recover for at least 2 weeks before imaging. To image, CX3CR1$^{GFP/+}$ mice were placed on a Kopf sterotax with heating pad and were anesthetized with isofluorane (1.5%). Imaging was performed 0–200 μm below the surface of the somatosensory cortex. Vessels were labeled by an intraperitoneal (IP) injection of Rhodamine B (Sigma, CAS 81-88-9, 50-100uL of 1 mg/mL). Optical sections were acquired using a Leica SP8 multiphoton microscope with a coherent laser. A wavelength of 880 nm was used to image microglia, and images were collected at a 1024 x 1024 pixel resolution using a 25 x 0.9 NA objective with a 1.5x optical zoom. Several fields of view of z stack images were collected through a volume of tissue. To observe microglial dynamics, z stack time-lapse images were acquired every minute at 2 μm steps. Z projections of longitudinal multiphoton videos were created and analyzed using Fiji.

QUANTIFICATION AND STATISTICAL ANALYSIS

Sholl analysis of microglial morphology for ramification index

The ramification of microglial processes was determined using a Sholl analysis through the SNT plugin in ImageJ. Slices including the hippocampus (the CA1 region) and the cortex were stained for Iba1 to identify microglia. Microglia from 3 to 5 non-overlapping fields of view and displayed well-defined bodies and processes were randomly selected from each mouse. After using a custom segmentation plugin with Ilastik, the images were converted to 8-bit grayscale and a binary threshold to identify individual cells. The Sholl analysis plugin plotted concentric circles 1 μm apart and determined the number of microglial branch intersection points for each circle. The Sholl analysis parameters of total intersection and the ramification index were determined from exported datasets analyzed in R. The data was analyzed using a one-way ANOVA after checking residuals to determine difference between groups.

Quantification of cFos fluorescence intensity

To quantify neuronal activation reflected by c-Fos labeling, mean fluorescence intensity in the CA1 and cortex was determined. The images were converted to 8-bit grayscale and had background fluorescence subtracted via the Subtract Background feature in ImageJ. Mean fluorescence intensity in each ROI had background fluorescence intensities in surrounding areas subtracted to provide a normalized value. Three sections were analyzed per mouse, which were averaged to give one mean fluorescence intensity value per one biological sample.

Ilastik-based quantification of VGAT area

VGAT IHC was analyzed in a pixel-classification pipeline in Ilastik (https://www.ilastik.org) then transferred to ImageJ. High-resolution TIFF files encompassing both CA1 and cortical regions were loaded into Ilastik's Pixel Classification module. The classification model differentiated VGAT labeled puncta and nonspecific labeling (background). Classifications were exported as 8-bit TIFF files and were then thresholded in Fiji and rendered as a binary mask. ROIs for CA1 and the cortex were manually isolated as regions of interest and percent area filled with VGAT or VGLUT labeling within each region was measured in Fiji's Measure tool. Three sections were analyzed per mouse and the average area per animal was then used as one biological sample for statistical comparison.

Statistical analysis

Data were initially measured for normality and homoscedasticity and upon comparing normal distributions and variances further analyzed with the respective tests. Student's *t* test was used to compare two-groups and one- or two-way ANOVA used to compare more than two groups. The level of significance was determined with p values as follows: $^{*}p < 0.05$; $^{**}p < 0.01$; $^{***}p < 0.001$; and $^{****}p < 0.0001$. Specific tests are stated in the figure legend for each of the experiments.